International Journal for Housing Science and Its Applications

Publish September 8, 2025. Volume 47, Issue 1 Pages 124-137

https://doi.org/10.70517/ijhsa47110

Visualization Research of Sports Rehabilitation Training System Based on Brain-Computer Interface with Artificial Intelligence Support

Yun Jiang[1,*]

[1] Police Practical Combat College of Guangxi Police College, Nanning, Guangxi, 530000, China

Corresponding authors: (e-mail: jy13207818858@163.com).

Abstract Brain-computer interfaces (BCIs) are an emerging human-machine interface technology that establishes a direct connection between the human brain and machines, thereby offering significant application potential in the field of sports rehabilitation training. This paper focuses on the overall control scheme design of a sports rehabilitation training system, which primarily consists of three components: the host computer, the underlying motion control system, and detection feedback. Magnetic control damping force is incorporated to enhance muscle strength in the patient's injured limb. In terms of rehabilitation training action matching, preprocessing of electroencephalographic (EEG) signals is performed by removing baseline drift, power frequency interference, and electrooculographic (EOG) interference. Additionally, for the traditional dynamic time warping (DTW) algorithm, a similarity measurement method tailored to the specific requirements of rehabilitation training action matching is introduced to impose temporal constraints on the matching points of two action sequences. This leads to the proposal of an improved DTW algorithm for efficient matching and recognition of rehabilitation training actions. Furthermore, based on the proposed rehabilitation training action matching model, an evaluation method and scoring formula for rehabilitation training actions are proposed. The designed rehabilitation training action matching model achieves an identification accuracy rate of 79.00% or higher for three randomly selected matching action groups.

Index Terms sports rehabilitation training, action matching, EEG signals, action evaluation, dynamic time warping algorithm, brain-computer interface

I. Introduction

In recent years, the number of patients with limb motor dysfunction caused by diseases such as stroke, spinal cord injury, or neurogenic muscular atrophy has been steadily increasing. This not only severely impacts patients' daily lives and work but also increases their psychological burden [1]-[4]. Therefore, developing scientifically feasible rehabilitation training programmes for these patients is of great significance. Sports rehabilitation training refers to physical activities conducted under professional guidance to facilitate the recovery or improvement of motor function after it has been impaired [5]. The feasibility of rehabilitation training stems from the plasticity of the nervous system, which can adaptively adjust neural circuits and synaptic structures in response to changes in the external environment. Appropriate rehabilitation therapy is effective in restoring neural and motor function [6]-[9]. However, traditional clinical rehabilitation training has certain drawbacks, including high physician workload, monotonous rehabilitation processes, poor patient engagement, and training outcomes influenced by physician subjective judgement, leading to suboptimal rehabilitation outcomes [10]-[12]. With economic development and the application of artificial intelligence technology in the medical field, patient rehabilitation training systems are gradually shifting toward intelligentisation.

Brain-computer interface (BCI) technology is a technique that enables direct communication between the human brain and machines [13]. As a novel human-machine interaction technology, it holds significant application potential across various fields, including medicine, healthcare, entertainment, and industry [14], [15]. In the field of rehabilitation therapy, compared to traditional treatment methods, novel rehabilitation training methods using brain-computer interface technology can involve the brain's motor neurons in rehabilitation training, thereby more effectively promoting neural remodelling in the patient's motor cortex [16]-[19]. Additionally, novel rehabilitation training methods using brain-computer interface technology can alleviate the shortage of rehabilitation therapists and the time-consuming and labour-intensive nature of manual rehabilitation [20], [21]. Furthermore, BCI technology holds great potential in the field of medical care [22]. By assisting

patients in controlling various external devices, such as wheelchairs, robotic arms, and smart home appliances, BCI technology can bring significant convenience to disabled patients and greatly reduce the burden of care [23]-[25]. In the future, as the Internet of Things becomes widespread, integration with BCI technology will open up endless possibilities for patients [26], [27]. Therefore, in the future IoT era of interconnected devices and intelligent interaction, brain-computer interface technology, with its unique properties, will undoubtedly drive the field of motor rehabilitation training to new heights of brilliance.

Currently, brain-computer interface (BCI) technology plays a crucial role in rehabilitation training and is increasingly gaining recognition. Identifying patients' motor intentions through electroencephalographic (EEG) or electromyographic (EMG) signals and using them as commands to control rehabilitation scenarios has become one of the key research areas. Liao, W, and colleagues conducted a comparative analysis of the efficacy differences between motor imagery brain-computer interface (MI-BCI) combined with physical therapy and physical therapy alone for motor rehabilitation training in patients with ischemic stroke. They found that the MI-BCI system has the feasibility of actively inducing neural rehabilitation, effectively improving patients' motor function, and thereby enhancing rehabilitation training outcomes [28]. Pichiorri, F et al. investigated the relationship between high-density cortical-muscular coherence (CMC) networks and upper limb movement deficits in stroke patients under the context of mixed-type brain-computer interface applications. Their experimental results provided data support for the optimisation and implementation of rehabilitation methods based on brain-computer interfaces [29]. Vourvopoulos, A., et al. developed the 'REINVENT' platform, which integrates virtual reality and brain-computer interface principles. This platform visualises patient-driven motor feedback, helping patients with varying degrees of motor impairments to establish sensory-motor pathways [30]. Saway, B. F. et al. designed invasive neuromodulation techniques to enhance the efficacy of conventional rehabilitation methods for stroke patients. The application of technologies such as brain-computer interfaces effectively alleviates persistent motor dysfunction in patients, and related AI-driven wearable devices also play a significant role in mitigating the impact of the disease [31]. Endzelytė, E, and colleagues investigated the impact of interventions combining brain-computer interface technology with occupational rehabilitation therapy on upper limb motor function and activities of daily living in subacute stroke patients, with the proposed integrated approach showing statistical significance [32]. Molinari, M and Masciullo, M demonstrated that neurobiological data collected by brain-computer interfaces can provide effective support for developing rehabilitation intervention measures tailored to patients' specific needs, holding significant research value for clinical applications [33]. Mrachacz-Kersting, N, et al. introduced the principle that activating neural ensembles in a coordinated manner enhances synaptic connections, and applied this to a brain-computer interface rehabilitation therapy system. By designing rehabilitation protocols that precisely couple brain commands with incoming signals, this approach is crucial for driving clinical and neurophysiological changes in patients [34]. Lin, B. S. et al. developed a motor rehabilitation training system integrating motion tracking devices (MTD), portable electroencephalography (EEG) devices, and interactive virtual reality (VR) games, utilising EEG signal data collected via brain-computer interfaces to enhance the system's motor function recovery efficacy [35]. With the support of virtual reality technology, brain-computer interface technology can effectively enhance patients' motivation for rehabilitation training, thereby promoting the activation of neurons with residual function. Meanwhile, the designed targeted rehabilitation training programme can meet the rehabilitation training needs of patients at different stages, which is of great significance.

This paper first outlines the overall architecture and control scheme of a sports rehabilitation training system, with a focus on the operational principles and calculation methods of magnetic-controlled damping force. Secondly, in the preprocessing of electroencephalogram (EEG) signal data, the paper separately analyses methods for correcting baseline drift, filtering out power frequency interference, and removing eye movement artifacts. Additionally, a traditional action time alignment algorithm is introduced as an action matching and recognition algorithm, with improvements made to its similarity measurement method and time alignment, to establish an action matching model for rehabilitation training based on brain-computer interface (BCI). Based on this action matching model, evaluation methods for single and combined rehabilitation actions are designed. Furthermore, by combining the time-domain characteristics of motor cortex-related potentials, we analyse the changes in EEG signal potentials for different rehabilitation training actions. Finally, we conduct model training, evaluate the effectiveness of the proposed rehabilitation system, and verify its accuracy.

II. Design of a control scheme for a sports rehabilitation training system

II. A. System Control Plan

When introducing the overall structure of the system, it is divided into an upper limb rehabilitation system and a lower limb rehabilitation system, which are mutually independent and do not interfere with each other. From the perspective of the functions the system achieves, both the upper and lower limb systems require independent operation of the left and right limbs in brain-controlled mode. Therefore, the entire system has four independent degrees of freedom, with two degrees of freedom each in the upper and lower limb systems. Regarding the system's actuators, the upper limb system achieves separation of the left and right sides by controlling two stepper motors, while the lower limb system is connected by two

electromagnetic clutches and one stepper motor. The independent operation of the two sides is achieved by controlling the engagement state of the clutches. In terms of control methods, both the upper limb system and the lower limb system utilise distributed control to achieve independent operation of both sides in brain-controlled mode. In other modes, after the left and right wheels are coaxial, the system employs centralised control to achieve synchronised operation of both sides. For the entire system, a combined control method of distributed and centralised control is adopted, meaning that either the upper limb system or the lower limb system can be operated independently, or both systems can be operated simultaneously. This control method enhances the system's flexibility while ensuring more stable operation.

The overall control scheme for the upper and lower limb rehabilitation system based on brain-computer interface technology is shown in Figure 1. The system consists of three parts: the host computer, the lower-level motion control system, and the detection and feedback system.

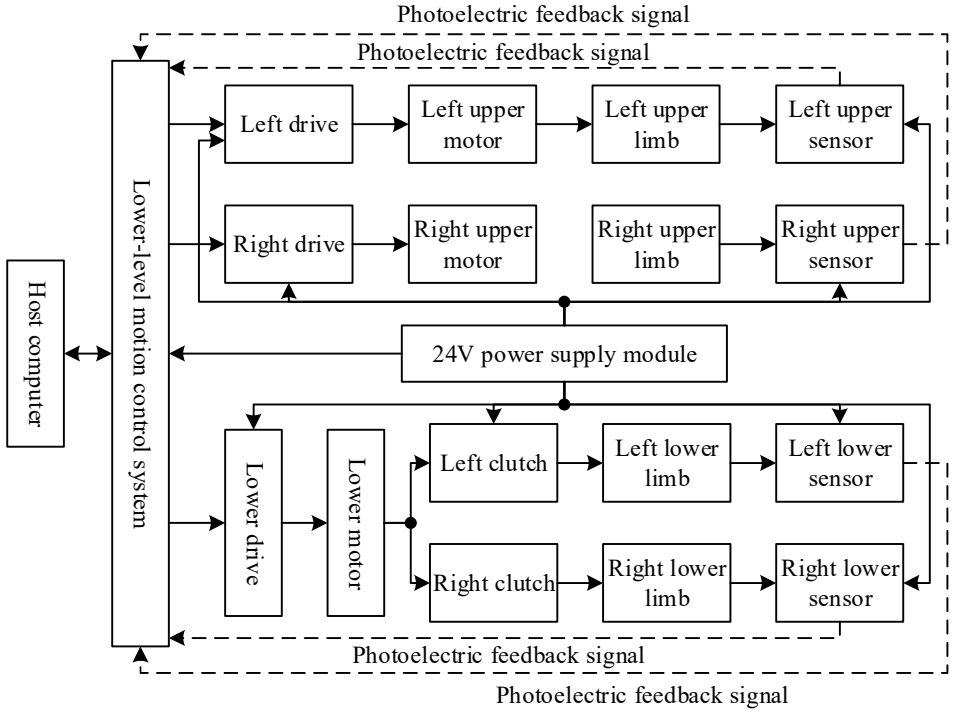

Figure 1: Overall system control scheme

II. B. Magnetic control damping force

To improve muscle strength in the patient's injured limb, the system incorporates a damping design during active rehabilitation training. Utilising magnetic control damping principles, the rehabilitation system has five damping force settings. During training, patients can select different damping levels according to their muscle strength to help the injured limb undergo muscle strength training.

II. B. 1) Design Principles

The principle of magnetic resistance generation is shown in Figure 2. Six sets of magnetic components (non-contacting with the flywheel) are installed on the outer side of the flywheel. When the rehabilitation vehicle moves, it drives the flywheel to rotate together. The conductive layer of the flywheel cuts through the magnetic field lines to generate current, and the magnetic field exerts a force on the charged conductor. To more intuitively describe the process of magnetic control damping force generation, we simplify the magnetic field of the external magnetic control wheel into a simple model and treat the conductive layer as composed of countless fine wires. When the conductor cuts through the magnetic field lines, eddy currents are generated, as shown in Figure 2. The magnetic field then exerts a Lorentz force on the moving conductor. According to the Lorentz force direction determination rule (left-hand rule), all instantaneously generated Lorentz forces are determined to be opposite to the direction of the flywheel's motion, thereby generating magnetic control resistance.

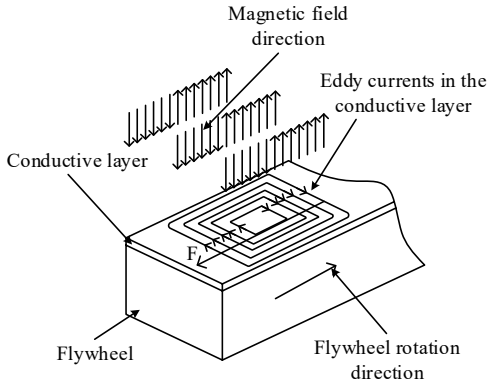

Figure 2: The principle of magnetic control resistance generation

The formula for the Lorentz force is

$$F = Bqv \tag{1}$$

In the formula:

F ——Lorentz force, i.e., the magnitude of the magnetic control damping force;

B ——magnetic induction intensity, related to the magnetic field intensity on the surface of the magnet assembly and the magnetic gap;

q ——charge of the charged particle;

v ——velocity of the charged particle.

The Ampere force is the macroscopic manifestation of the Lorentz force and can be derived by reversing the Lorentz force formula. The Ampere force formula is

$$F = BIL \tag{2}$$

In formula (2), I represents the induced current generated by the conductor cutting the magnetic field lines, and L represents the length of the conductor. In practical applications, the Lorentz force is usually replaced by the Ampere force.

II. B. 2) Calculation method

Assuming that the magnetic field induction strength of the external magnetic control wheel is B, a set of magnet components is selected for magnetic control resistance analysis, denoted as component A. The angular velocity of the flywheel is set to ω, the distance from the inner diameter of the conductive layer to the centre is r_1, the distance from the outer diameter to the centre is r_2, and the thickness of the conductive layer is h.

The conductor cutting the magnetic field lines is abstracted as a conductor rod of length L, and it is assumed that the flywheel rotates in a uniform magnetic field. A simplified model is shown in Figure 3. When the conductor rod moves through the magnetic field component A, cutting the magnetic field lines, the induced electromotive force generated radially is equal, and the resistance value of the eddy current circuit is also equal.

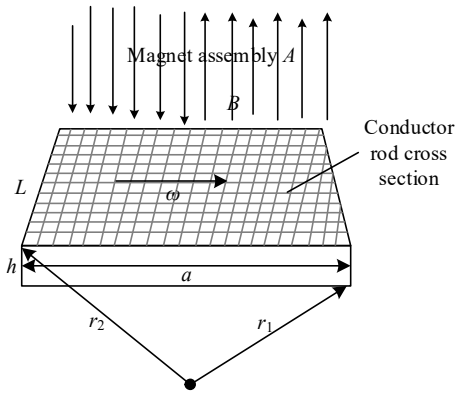

Figure 3: Simplified model of an abstract conducting rod cutting magnetic field lines

Here, we perform a simple formula derivation and calculation based on the conditions that the conductor cuts the magnetic field lines at a speed of v, the magnetic induction intensity is in the B direction, and the conductor rods are perpendicular to each other. In practical applications, if they are not perpendicular to each other, the corresponding formula calculation can still be performed using their equivalent components in the perpendicular direction. The induced electromotive force generated by the conductor rod cutting the magnetic field lines is denoted as

$$E = BLv \tag{3}$$

In the formula, $v = \omega * r$ and r represent the radius of rotation of the conductor. If the conductor rod is regarded as a collection of countless points, then the speed of movement of each point on r_1 to r_2 when cutting the magnetic field lines will be different. Here, the rotational speed at the centre of the conductor rod is used for calculation, i.e. $r = r_1 + h/2$. Let the equivalent resistance of the system be R. In the equivalent circuit, according to Ohm's law, the induced current is obtained as

$$I = \frac{E}{R} = \frac{BL\omega}{R} r \tag{4}$$

The formula for calculating equivalent resistance is

$$R = \rho \frac{L}{S} \tag{5}$$

Among these, ρ represents the resistivity of the copper conductor, which is $0.0172\Omega m$ at standard atmospheric pressure; S represents the cross-sectional area of the conductor, which is expressed as $S = h * a$ in the abstract model of the conductor rod; and a represents the length of a set of magnet components. Substituting these values, we obtain

$$I = \frac{BS\omega}{\rho} r \tag{6}$$

During system operation, the units are n and $r/\min$. According to the angular velocity calculation formula, and after conversion to a unified standard unit, the result is

$$\omega = 2\pi n / 60 \tag{7}$$

Finally, based on the Ampere force formula, we derive the magnetic control resistance.

$$F = BIL = \frac{Larh\pi}{30\rho} B^2 n \tag{8}$$

From formula (8), it can be seen that, when all parameters remain unchanged, the magnitude of the magnetic control force is only related to the magnetic field strength and the operating speed of the system. The magnetic field strength is related to the magnetic gap; the smaller the magnetic gap, the greater the magnetic field strength. In practical applications, when the operating speed of the system is constant, the magnitude of the magnetic field strength can be changed by adjusting the magnetic gap, thereby regulating the magnitude of the magnetic control resistance.

III. Action matching model for rehabilitation training based on brain-computer interface

III. A. Preprocessing of electroencephalographic signals

III. A. 1) Removal of baseline drift

There are many methods for baseline drift correction, with the most commonly used ones including the following: moving average method, least squares method, and median filtering method. Compared to the latter two methods, the moving average method has distinct advantages: it is convenient and quick, has good real-time performance, and can perform complete calculations on the data. Based on this, this paper selects the moving average method to remove baseline drift from EEG signals. The specific method is as follows:

First, select an appropriate window size for the data to be processed. Within the window range, there may be abnormal data values that need to be handled. Here, the average value is calculated. Then, perform a moving window operation and repeat the averaging calculation until all the data to be processed has been calculated.

Select a data segment $y(i)$, $i = 0,1,\cdots,n$ set the window length to $N\left(N < n/2\right)$, calculate the average value of the data $y(0) \sim y(N)$ within the window, and obtain $y_1(0)$. Then, set p as the step size, continue to move the window, and obtain the abnormal value at the centre point. Perform curve fitting to obtain $y_1(l), l = 0,1,\cdots,m$. The moving step size p and the length of the fitted curve data m have a certain relationship, i.e., $l = (n-N)/p$, and rounding is performed. Finally, the

fitted curve is upsampled to obtain $y_1(i)$, $i = 0,1,\cdots,n$.

The preprocessed signal can be obtained by subtracting the abnormal fitted curve value from the original data value:

$$y_m(i) = y(i) - y_1(i), i = 0,1,\cdots,n \tag{9}$$

III. A. 2) Removal of power frequency interference

This paper employs an adaptive 50Hz filter to remove power frequency interference from electroencephalogram (EEG) signals. The process primarily involves subtracting the reference artifact component from the observed signal containing artifact components, followed by analysis based on the minimum mean square error criterion. The key lies in dynamically estimating the artifact components of the input signal.

To achieve better filtering performance, it is necessary to enable the filter coefficients to automatically adjust accordingly, thereby maximising the removal of artifacts and preserving the useful signals. The design principle of the adaptive filter is shown in Figure 4. The output of the adaptive filter $y(i)$ is:

$$y(i) = w(i)^T x(i) \tag{10}$$

The expected output signal $\varepsilon(i)$ is:

$$\varepsilon(i) = s(i) - y(i) \tag{11}$$

The iterative formula for the power coefficient is:

$$w(i+1) = w(i) + \beta\varepsilon(i)x(i) \tag{12}$$

In the formula, β is the global stride.

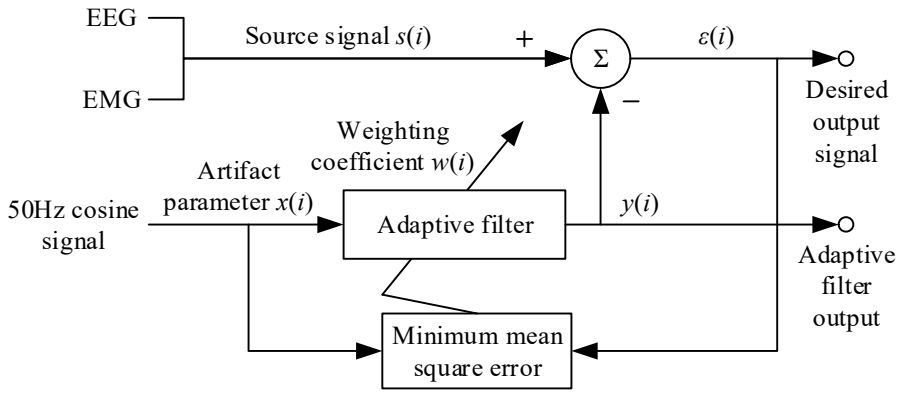

Figure 4: Principle of Adaptive Filter

III. A. 3) Removal of eye movement interference from EEG

During EEG data collection, participants may blink, and this action can generate electrooculographic (EOG) artifacts that may adversely affect experimental results. The system described in this paper employs Independent Component Analysis (ICA) to filter out eye movement artifacts, which is a blind source separation algorithm. This method gained recognition in the mid-1990s, with studies demonstrating that ICA can effectively remove eye movement artifacts from EEG signals.

Suppose the observed N-dimensional signal is $X(t) = [x_1(t), x_2(t), \cdots, x_n(t)]$, and the $S(t) = [s_1(t), s_2(t), \cdots, s_m(t)]$-dimensional source signal is M, where the source signal $S(t)$ can be mixed with an unknown matrix A to form the desired observed signal $X(t)$, i.e., $X(t) = A * S(t)$. Solving for the separation matrix W is the core idea of this method, with the goal of making the output signal $U(t) = W * X(t)$ as similar as possible to the source signal $S(t)$. The optimal separation matrix is the one that, after separation, makes the desired output signal $U(t)$ achieve the maximum non-Gaussianity of the separation matrix W.

III. B. Improving the dynamic time warping algorithm

Motion matching and recognition, as one of the hot research areas in computer vision, has been widely applied in fields such as video surveillance and human-computer interaction. Due to the professional and special nature of the application scenarios in rehabilitation training systems, motion matching is achieved by comparing standard template motion videos recorded by rehabilitation therapists with patients' rehabilitation training videos to enable motion recognition. Therefore, the primary

motion matching algorithms that can be selected include CRF, HMM, and DTW. Among these, probability-based algorithms such as CRF and HMM require prior modelling for action recognition. When actions are complex, the algorithm's complexity increases. Additionally, since the rehabilitation training system's action assessment requires calculating the similarity values between the patient's action samples and the standard template actions, CRF and HMM are not well-suited for this system in such cases. Therefore, this chapter selects the Dynamic Time Warping (DTW) algorithm for action matching and recognition.

The DTW algorithm effectively addresses the issue of motion anticipation and lag between rehabilitation training actions and standard template actions during patient rehabilitation training, i.e., the mismatch between two action sequences on the time axis. DTW calculates the similarity value between two action sequences by outputting the optimal alignment value between two curves, i.e., the minimum cumulative distance. The smaller the cumulative distance, the closer the two action sequences are, and the better the rehabilitation training actions match.

III. B. 1) Similarity measurement based on limb division

The DTW algorithm can effectively match patient rehabilitation training movements with standard template movements. However, in actual practice, there are special circumstances, such as when patients have not yet regained the ability to stand and may be seated in a chair or on a bed during rehabilitation training. Patients may use assistive devices for rehabilitation training, such as crutches or parallel bars for standing. These special circumstances can interfere with the matching of rehabilitation training movements, and rehabilitation therapists cannot capture all possible scenarios in standard template videos during filming. Therefore, it is necessary to address this issue through algorithmic solutions.

To address this, this chapter proposes a new similarity measurement method based on limb segmentation. Rehabilitation training movements primarily focus on improving the mobility of the human limbs. The key skeletal points of the human body can be divided into four regions: the left and right upper limb regions and the left and right lower limb regions. By calculating the average joint movement amplitude of each region, we can determine whether the region is participating in rehabilitation training movements. The formula for calculating the average joint movement amplitude within each region is shown in Equation (13).

$$Amp_r = \frac{\sum_i \max(x_i) - \min(x_i)}{\sum_i 1} \tag{13}$$

In this context, Amp denotes the average joint movement amplitude within the region, r denotes the r region among the four limb regions, i denotes the i joint within the r limb region, $\sum_i 1$ represents the total number of joints in the r limb region, and the range of values for i encompasses all joints contained within the r limb region. x_i denotes the joint activity angle of the i joint within the r limb region.

Based on the Euclidean distance in the traditional DTW algorithm, a similarity measurement method that satisfies the special characteristics of rehabilitation training motion matching is proposed, with the specific formula shown in Equation (14).

$$\begin{cases} E_r = 0, & Amp_r < T \\ E_r = \sqrt{\sum_i (x_i - y_i)^2}, & Amp_r > T \\ d = +\infty, & F_{test} \neq F_{standard} \\ d = +\infty, & \sum_r E_r = 0 \\ d = \dfrac{\sum_r E_r}{\sum_r 1}, & F_{test} = F_{standard} \end{cases} \tag{14}$$

Among these, d represents the result of the similarity calculation, and T is the manually set threshold for determining whether a limb region participates in rehabilitation training exercises. When $Amp < T$, it indicates that this region does not participate in the current rehabilitation training treatment, i.e., this region is deemed similar by default. $Amp > T$ calculates the similarity value between this region and the standard template action. i represents the i joint in the r limb region, with i ranging over all joints in the r limb region. x_i denotes the angle of the i joint in region r of the patient's rehabilitation training action, and y_i denotes the angle of the i joint in region r of the standard template action. E_r is the calculated Euclidean distance value, F_{test} is the orientation between the patient's rehabilitation training action and the camera, $F_{standard}$ is the orientation between the standard template action and the camera, and $\sum_r 1$ denotes the total

number of limb regions.

III. B. 2) Adding time constraints

In practice, it has been found that while the DTW algorithm solves the problem of two action sequences not being aligned on the time axis, it also presents new challenges. If the matching points on the two action sequences are too far apart, the matching results are often inaccurate. To address this issue, a time constraint has been added to the traditional DTW algorithm: a threshold T is set, and the matching points on the two action sequences must satisfy equation (15).

$$|i-j| \le T \tag{15}$$

In this context, i represents the i frame of the patient's rehabilitation exercise sequence, j represents the j frame of the standard template action sequence, and $|i-j| \le T$ indicates that the difference between all matching frames of the two action sequences is less than T. For example, when the threshold is $T = 60$, it means that the i frame of the patient's rehabilitation training can only be matched with the standard template action sequence within 60 frames before and after the i frame. If converted to time, when the human posture estimation algorithm runs for $FPS = 20$, it means that the action at the i moment of the patient's rehabilitation training can only be matched with the standard template action at the i moment within 3 seconds before and after.

IV. Rehabilitation movement assessment method based on movement matching

IV. A. Assessment of individual rehabilitation exercises

Based on the expertise of rehabilitation exercise specialists, a new assessment method for rehabilitation exercises has been designed. First, according to the exercise scoring tables, such as the abduction scoring table in the shoulder joint Constant scoring table, rehabilitation therapists should film standard template videos corresponding to the angle ranges for each scoring segment and assign corresponding scores to each standard template video, i.e., label the standard template videos with the exercise name and score. Then, using the movement matching method proposed in Chapter 3, the scores of the standard template movements with the highest similarity are obtained as a reference score for rehabilitation exercise assessment. The matched template, along with the templates one level higher and one level lower in score, are used as evaluation references for the rehabilitation exercise assessment method. A rehabilitation exercise scoring formula is designed, as shown in Equation (16).

$$\begin{cases} \Phi_i = \max(x_i) - \min(x_i) \\ f(\Phi_i) = \begin{cases} \dfrac{\Phi_i - \Phi s_i}{a_i} & , \Phi s_i \le \Phi_i \le \Phi s_i + a_i \\ \dfrac{\Phi s_i - \Phi_i}{b_i} & , \Phi s_i - b_i \le \Phi_i < \Phi s_i \end{cases} \\ J = \begin{cases} \sum_i \left(\dfrac{f(\Phi_i)}{\sum_i f(\Phi_i)} \times f(\Phi_i) \right), \sum_i f(\Phi_i) \ne 0 \\ 0, \sum_i f(\Phi_i) = 0 \end{cases} \\ F = \begin{cases} \dfrac{\sum_i \left(\delta(D_i < D_\tau) \times (G + J \times g_{ip}) \right)}{\sum_i 1} & \Phi s_i \le \Phi_i \le \Phi s_i + a_i \\ \dfrac{\sum_i \left(\delta(D_i < D_\tau) \times (G - J \times g_{down}) \right)}{\sum_i 1} & \Phi s_i - b_i \le \Phi_i < \Phi s_i \end{cases} \end{cases} \tag{16}$$

Among these, F represents the score for a single action, Φ_i denotes the amplitude of the i joint angle in the rehabilitation training action, Φ_{S_i} denotes the amplitude of the i joint angle in the standard template action obtained through matching, a_i represents the difference between the amplitude of the i joint angle in the standard template action obtained through matching and the amplitude of the i joint angle in the standard template action with a higher base score, b_i represents the difference between the amplitude of the i joint angle of the matched standard template action and the i joint angle of the standard template action with a lower baseline score, $f(\Phi_i)$ represents the proportional relationship between the difference in amplitude between the i joint angle of the current action and the i joint angle of the standard template action with a higher or lower baseline score, J is the weighted sum of $f(\Phi_i)$, The weight of the i joint is the proportion of $f(\Phi_i)$ out of the total sum of all $f(\Phi_i)$, G is the reference score of the matched standard template action,

and g_{down} is the difference between the base score of the matched standard template action and the base score of the lower-level base score, g_{up} is the difference between the baseline score of the matched standard template action and the baseline score of the higher-level baseline, When $D_i < D_T$, it indicates that there is a standard template action matching the rehabilitation training action; when $D_i > D_T$, it indicates that there is no standard template action matching the rehabilitation training action, and the action is; $\delta(D_i < D_T)$ indicates that if $D_i < D_T$ holds, then $\delta(D_i < D_T) = 1$, otherwise $\delta(D_i < D_T) = 0$.

Specifically, the first step in the rehabilitation training assessment method is to determine whether the rehabilitation training movements have corresponding standard template movements. If there are no corresponding standard template movements, the movements are deemed non-standard and receive a score of 0. If there are corresponding standard template movements, the reference score obtained from the matched standard template movements is used as the baseline score for further calculations; The second step involves calculating the amplitude of each joint angle during the patient's rehabilitation training, the difference ratio between the standard template action that matches it, the standard template action with a base score one level lower than the matched standard template, and the standard template action with a base score one level higher than the matched standard template, and then calculating the weighted sum of all joint angle amplitudes; Step 3: If the actual amplitude is less than the amplitude of the matched standard template action, subtract the base score from the product of the weighted sum from Step 2 and the difference between the base scores of the matched standard template action and the standard template action with a base score one level lower. If the actual amplitude is greater than the amplitude of the matched standard template action, add the base score to the product of the weighted sum from Step 2 and the difference between the base scores of the matched standard template action and the standard template action with a base score one level higher.

IV. B. Comprehensive assessment of a set of actions

During treatment, patients often undergo training through a set of rehabilitation exercises. Therefore, it is also necessary to conduct research on the overall evaluation of a set of exercises, using the average value of the sum of the scores for all individual exercises as the evaluation standard. The scoring formula for a set of exercises is given by Equation (17).

$$F_{total} = \frac{\sum_t F_t}{\sum_t 1} \tag{17}$$

In the formula, F_{total} represents the comprehensive score for a set of rehabilitation exercises, t represents the t exercise in a set of rehabilitation exercises, $\sum_t 1$ represents a total of t exercises, and F_t represents the score for the t exercise in a set of rehabilitation exercises.

V. Analysis of sports rehabilitation training based on brain-computer interfaces

V. A. Analysis of motor-related cortical potentials

Motor-related cortical potentials (MRCPs) have very low-frequency components (0.05–3 Hz) and are associated with motor imagery and motor execution. MRCPs exhibit distinct temporal domain characteristics in electroencephalograms (EEGs), as shown in Figure 5. Specifically, a negative deflection is observed in the EEG 2 seconds before the onset of movement, representing cortical preparation for movement, followed by a rebound after the peak of maximum negativity. The negative deflection can be divided into the readiness potential (BP) and the motor potential (MP), which are respectively associated with the planning and execution of movement. The readiness potential (BP) has two components: early (BP1) and late (BP2), while the motor potential (MP) is associated with cortical activity during the later stages of movement preparation. The rebound following the peak of maximum negativity is referred to as the motor monitoring potential (MMP), which is associated with the outcome of the motor process following the execution of a motor intention on the contralateral sensorimotor cortex. It is generally believed that the readiness potential (BP) contains information about motor preparation, reflecting the intention to act, and can be observed even when the movement is not executed but merely imagined, thereby providing the possibility for motor intention detection.

This section focuses on analysing changes in brain electrical signals during preparation for sitting-to-standing transitions, laying the theoretical foundation for the practical application of the proposed rehabilitation training system and matching model. MRCP is closely related to the activation of various motor-related functional areas in the cerebral cortex during motor imagery and motor execution.

Ten participants were selected, and their electroencephalography (EEG) data from 2 seconds before the start of the movement to 3 seconds after the start of the movement were analysed. After preprocessing the EEG data for each participant, a Butterworth filter was applied to perform a low-pass filter at 3 Hz. The MRCP average values for each channel across all trials were then calculated for different movements. The FCz and Cz regions in the central sulcus of the sensorimotor cortex

were selected for analysis. The motor-related cortical potentials during movement execution for different movements are shown in Figure 6.

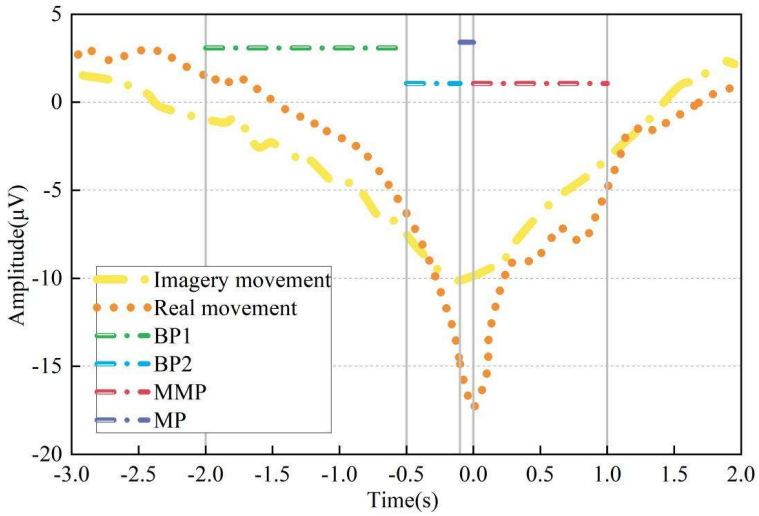

Figure 5: Exercise-related cortical potential

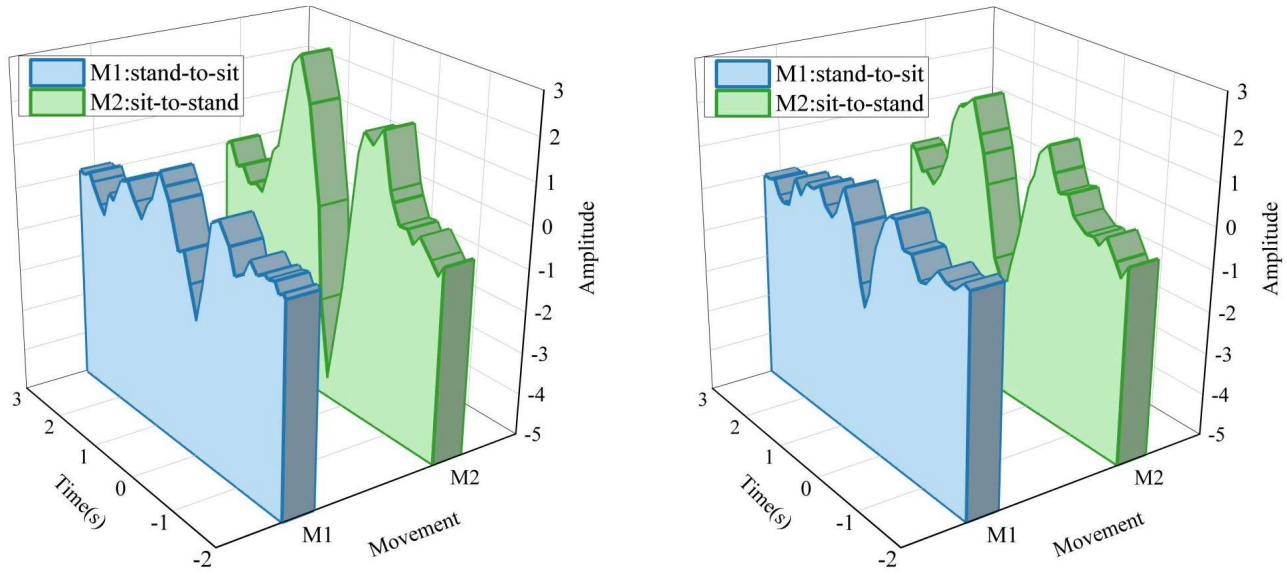

(a) FCz (b) Cz

Figure 6 Movement-related cortical potentials of different movements

For both the (M1) sitting-to-standing and (M2) standing-to-sitting movements, strong negative deflections can be observed. A downward trend begins approximately 550 milliseconds before the movement starts, reaching its peak when the movement begins. The brain activation patterns for the two movements exhibit a certain degree of similarity. From both channels, it can be seen that the motor-related cortical potentials for the standing movement have a larger amplitude than those for the sitting movement, indicating that neural activity in the cerebral cortex is more intense during the standing movement. The characteristic differences in MRCP between different movements provide another feasible channel for movement rehabilitation-type brain-computer interface systems.

The MRCP of the Cz channel under the two modes of motor imagery and motor execution for the two actions of standing up and sitting down are shown in Figure 7. It can be seen that a negative shift in the low-frequency band of the electroencephalogram signal also occurs before the motor imagery of the action. Regardless of whether it is the action of standing up or sitting down, the amplitude of the MRCP during motor imagery is smaller than that during actual motor

execution, indicating that the two modes have similar brain activation but differ in activation levels, with motor execution mobilising more abundant resources in the relevant brain regions. Therefore, MRCP in motor imagery can also serve as another neural feature for motor intention recognition in brain-computer interfaces based on motor imagery.

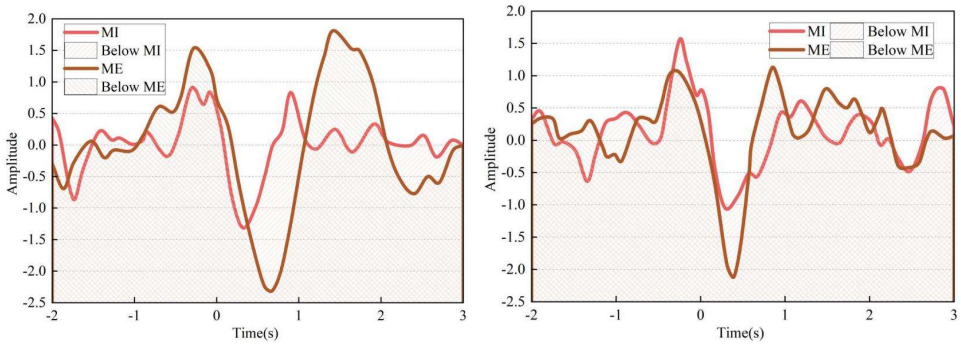

(a) Stand (b) Sit

Figure 7: Motor imagery and motor execution related to motor cortical potentials

V. B. Evaluation of Sports Rehabilitation Systems and Motion Matching Models

V. B. 1) Training the action matching model

Before training the model, it is necessary to filter the signals in the sample dataset. In the imagination experiment, although simple filtering and notch filtering were applied to the brain-computer interface device, due to the limitations of the device, parameters could not be freely adjusted, so further artifact removal was required. The collected EEG signals were filtered between 8 and 30 Hz to remove artifacts, as the primary signals from motor imagination are concentrated in this frequency band. The filtering results are shown in Figure 8, which compares the filtered and unfiltered signals from the C3 channel of a specific participant. Specifically: (E1) raw EEG signal, (E2) filtered EEG signal. It can be observed that after filtering, the EEG signal fluctuations become more regular, and the voltage range is concentrated within [-20, 20] μV.

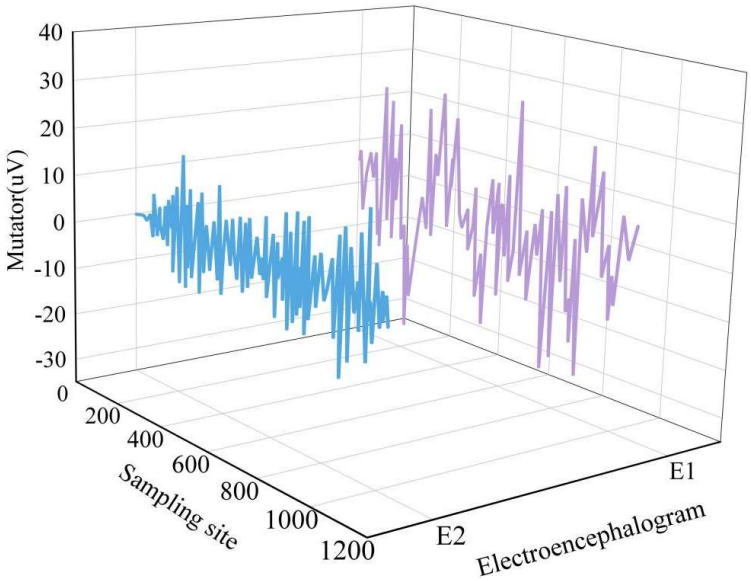

Figure 8: Comparison of C3 channel signal before and after filtering

V. B. 2) Testing the effectiveness of rehabilitation systems

To validate the effectiveness of the designed rehabilitation system, this study arranged for one participant to use the system in practice to verify its reliability. After data collection and filtering, 150 data sets were ultimately obtained to establish the training set, and 50 actual rehabilitation training test experiments were conducted. After each rehabilitation training movement, the actual movements and expected movements of the robotic arm were recorded for each test. Based on the experimental results, a confusion matrix was plotted as shown in Figure 9. The established rehabilitation training system

achieved an average accuracy rate of 72.00% or higher for EEG signal recognition. The recognition accuracy rates for the user's 'left' (>90.0%), "right" (>70.0%), and 'up' (>70.0%) commands were all relatively high. Due to the participants' confusion regarding the imagination task for the 'down' action, the control effect was poor, resulting in an intention recognition accuracy rate of only >45.00% for the 'down' action.

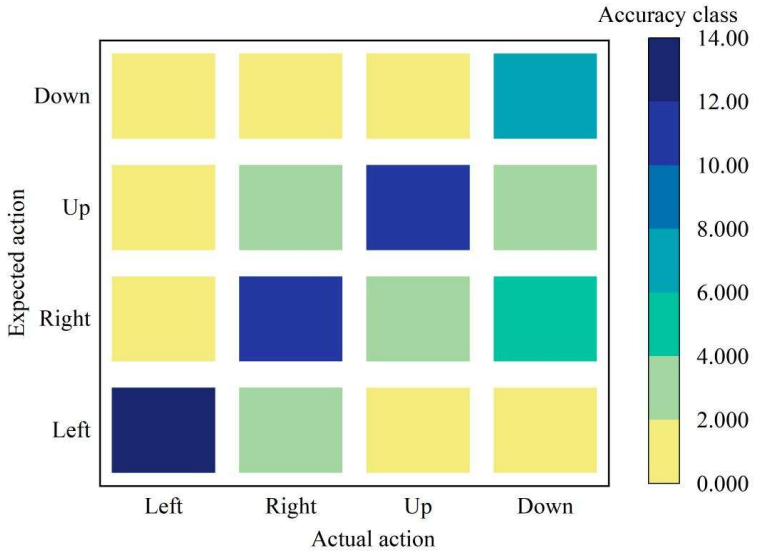

Figure 9: The confusion matrix of rehabilitation training experiments

V. B. 3) Testing experiments for algorithm accuracy

Randomly select 3 matching actions: (1) 'T' shape to raising both hands; (2) "T" shape to rotating the forearms upward; (3) 'T' shape to placing both hands on the hips. The accuracy of the improved Dynamic Time Warping (DTW) algorithm after 30 experiments is shown in Figure 10. A total of 90 experiments were conducted for the three actions, with an overall accuracy rate of 79.00% or higher, indicating that the overall accuracy of the designed improved DTW algorithm is relatively high.

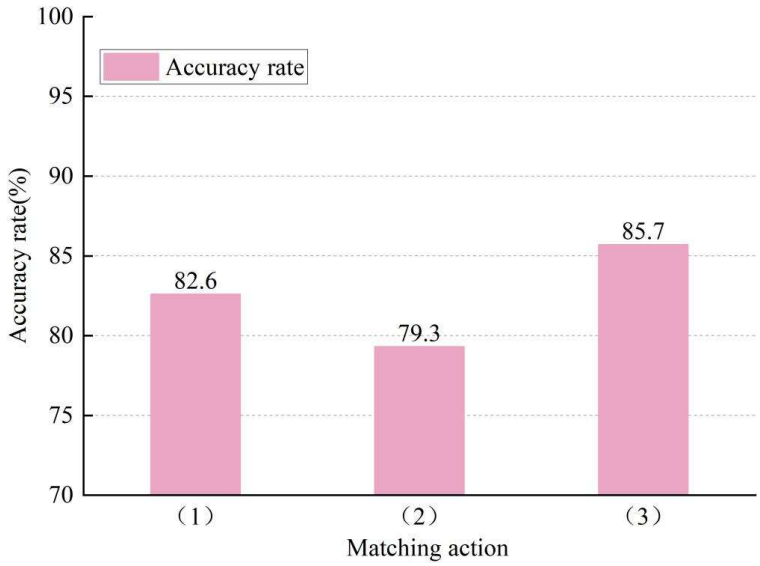

Figure 10: The algorithm accuracy rate of the matching action

Three types of patient motion streams and standard motion streams were selected to test algorithm accuracy based on error conditions: 1–10 frames, 10–20 frames, and over 20 frames. The results of the algorithm accuracy test are shown in Table 1. It can be seen that, overall, the algorithm's recognition accuracy improves as the motion stream error decreases. When the motion sequence error exceeds 20 frames, the algorithm accuracy rate is only 42.3%, while when the motion sequence error

is controlled within 1–10 frames, the algorithm accuracy rate reaches 92.7%. Based on this, the duration of patient motions and standard motions in the rehabilitation training system should be as close as possible.

Table 1: The algorithm accuracy of the action flow situation

Stream of action	Action times	Accuracy rate (%)
1 to 10 frames	15	92.7
10 to 20 frames	50	77.9
More than 20 frames	60	42.3

VI. Conclusion

(1) This paper divides the sports rehabilitation training system into two independent systems: the upper limb rehabilitation system and the lower limb rehabilitation system. By integrating distributed control and centralised control brain-controlled modes, the flexibility and stability of the system's operation are improved. In addition, magnetic control damping force is added to enhance the muscle strength of the patient's injured limbs.

(2) This paper establishes a brain-computer interface-based rehabilitation training action matching model by incorporating similarity measurement methods and time constraints into traditional dynamic time warping algorithms. Subsequently, comprehensive methods for single rehabilitation training actions and sets of actions are proposed for this action matching model. With the assistance of the proposed rehabilitation training action matching model, the average accuracy rate of the brainwave signal recognition in the designed rehabilitation training system is 72.00% or higher. The algorithm's recognition accuracy improves as the action flow error decreases, and when the action flow error is controlled within 1 to 10 frames, the algorithm's accuracy can reach as high as 92.7%.

This paper proposes a sports rehabilitation training system with high-precision motion matching and scientific evaluation, supported by artificial intelligence technologies such as brain-computer interfaces and motion matching models. It reduces the complexity of rehabilitation training and theoretically achieves the visualisation of sports rehabilitation training motions.

References

[1] Mameletzi, D., Anifanti, M., Baotić, K., Bernetti, A., Budinčević, H., Žuna, P. Č., ... & Kouidi, E. (2021). Identification of Good Practices in Long‐Term Exercise‐Based Rehabilitation Programs in Stroke Patients. BioMed research international, 2021(1), 9202716.

[2] Walsh, C. M., Gull, K., & Dooley, D. (2023). Motor rehabilitation as a therapeutic tool for spinal cord injury: New perspectives in immunomodulation. Cytokine & growth factor reviews, 69, 80-89.

[3] Demir, Y. P. (2017). Neuromuscular diseases and rehabilitation. Neurological physical therapy, 176-214.

[4] Kim, Y., Lai, B., Mehta, T., Thirumalai, M., Padalabalanarayanan, S., Rimmer, J. H., & Motl, R. W. (2019). Exercise training guidelines for multiple sclerosis, stroke, and Parkinson disease: rapid review and synthesis. American journal of physical medicine & rehabilitation, 98(7), 613-621.

[5] Xing, Y., Yang, S. D., Dong, F., Wang, M. M., Feng, Y. S., & Zhang, F. (2018). The beneficial role of early exercise training following stroke and possible mechanisms. Life sciences, 198, 32-37.

[6] Han, P., Zhang, W., Kang, L., Ma, Y., Fu, L., Jia, L., ... & Guo, Q. (2017). Clinical evidence of exercise benefits for stroke. Exercise for cardiovascular disease prevention and treatment: from molecular to clinical, part 2, 131-151.

[7] Lee, K. E., Choi, M., & Jeoung, B. (2022). Effectiveness of rehabilitation exercise in improving physical function of stroke patients: a systematic review. International journal of environmental research and public health, 19(19), 12739.

[8] Nie, J., & Yang, X. (2017). Modulation of synaptic plasticity by exercise training as a basis for ischemic stroke rehabilitation. Cellular and molecular neurobiology, 37(1), 5-16.

[9] van Duijnhoven, H. J., Heeren, A., Peters, M. A., Veerbeek, J. M., Kwakkel, G., Geurts, A. C., & Weerdesteyn, V. (2016). Effects of exercise therapy on balance capacity in chronic stroke: systematic review and meta-analysis. Stroke, 47(10), 2603-2610.

[10] Nikishina, V. B., Petrash, E. A., & Nikishin, I. I. (2019). Application of a hardware and software system of computer vision for rehabilitation training of post-stroke patients. Biomedical Engineering, 53(1), 44-50.

[11] Duan, R., Qu, M., Yuan, Y., Lin, M., Liu, T., Huang, W., ... & Yu, X. (2021). Clinical benefit of rehabilitation training in spinal cord injury: a systematic review and meta-analysis. Spine, 46(6), E398-E410.

[12] Panisset, M. G., Galea, M. P., & El-Ansary, D. (2016). Does early exercise attenuate muscle atrophy or bone loss after spinal cord injury?. Spinal cord, 54(2), 84-92.

[13] Peksa, J., & Mamchur, D. (2023). State-of-the-art on brain-computer interface technology. Sensors, 23(13), 6001.

[14] Cajigas, I., Davis, K. C., Meschede-Krasa, B., Prins, N. W., Gallo, S., Naeem, J. A., ... & Jagid, J. (2021). Implantable brain–computer interface for neuroprosthetic-enabled volitional hand grasp restoration in spinal cord injury. Brain communications, 3(4), fcab248.

[15] Robinson, N., & Vinod, A. P. (2016). Noninvasive brain-computer interface: decoding arm movement kinematics and motor control. IEEE Systems, Man, and Cybernetics Magazine, 2(4), 4-16.

[16] Yang, S., Li, R., Li, H., Xu, K., Shi, Y., Wang, Q., ... & Sun, X. (2021). Exploring the Use of Brain‐Computer Interfaces in Stroke Neurorehabilitation. BioMed Research International, 2021(1), 9967348.

[17] Ma, Y. N., Karako, K., Song, P., Hu, X., & Xia, Y. (2025). Integrative neurorehabilitation using brain-computer interface: From motor function to mental health after stroke. BioScience Trends, 19(3), 243-251.

[18] YuV, B., Ivanova, G. E., Stakhovskaya, L. V., & Frolov, A. A. (2019). Brain-computer-interface technology with multisensory feedback for controlled ideomotor training in the rehabilitation of stroke patients. hemispheres, 6, 11.

[19] Chaudhary, U. (2025). Neurotechnology in Stroke Rehabilitation: Innovations in Stroke Recovery and Neurotechnology. In Expanding Senses using Neurotechnology: Volume 2–Brain Computer Interfaces and their Applications (pp. 51-98). Cham: Springer Nature Switzerland.

[20] Sun, X., Li, M., Li, Q., Yin, H., Jiang, X., Li, H., ... & Yang, T. (2022). Poststroke Cognitive Impairment Research Progress on Application of Brain–Computer Interface. BioMed research international, 2022(1), 9935192.

[21] Kim, W. S., Cho, S., Ku, J., Kim, Y., Lee, K., Hwang, H. J., & Paik, N. J. (2020). Clinical application of virtual reality for upper limb motor rehabilitation in stroke: review of technologies and clinical evidence. Journal of clinical medicine, 9(10), 3369.

[22] Salsabila, O. (2025). RECENT TECHNOLOGICAL ADVANCEMENTS IN STROKE REHABILITATION: A SYSTEMATIC LITERATURE REVIEW ON INNOVATIONS, EFFECTIVENESS, AND IMPLEMENTATION IN PATIENT RECOVERY. Jurnal Kesehatan Saintika Meditory, 8(1), 67-90.

[23] Young, M. J., Lin, D. J., & Hochberg, L. R. (2021, April). Brain–computer interfaces in neurorecovery and neurorehabilitation. In Seminars in neurology (Vol. 41, No. 02, pp. 206-216). Thieme Medical Publishers, Inc..

[24] Wu, Q., Yue, Z., Ge, Y., Ma, D., Yin, H., Zhao, H., ... & Pan, Y. (2020). Brain functional networks study of subacute stroke patients with upper limb dysfunction after comprehensive rehabilitation including BCI training. Frontiers in Neurology, 10, 1419.

[25] Li, M., Xu, G., Xie, J., & Chen, C. (2018). A review: motor rehabilitation after stroke with control based on human intent. Proceedings of the Institution of Mechanical Engineers, Part H: Journal of Engineering in Medicine, 232(4), 344-360.

[26] Knežević, S. (2025). Brain-Computer Interfaces In Neurorehabilitation For Central Nervous System Diseases: Applications in Stroke, Multiple Sclerosis And Parkinson's Disease. Sanamed, 20(1).

[27] Rao, Z., Zhu, J., Lu, Z., Zhang, R., Li, K., Guan, Z., & Li, Y. (2024). A wearable brain-computer interface with fewer EEG channels for online motor imagery detection. IEEE Transactions on Neural Systems and Rehabilitation Engineering.

[28] Liao, W., Li, J., Zhang, X., & Li, C. (2023). Motor imagery brain–computer interface rehabilitation system enhances upper limb performance and improves brain activity in stroke patients: A clinical study. Frontiers in Human Neuroscience, 17, 1117670.

[29] Pichiorri, F., Toppi, J., de Seta, V., Colamarino, E., Masciullo, M., Tamburella, F., ... & Mattia, D. (2023). Exploring high-density corticomuscular networks after stroke to enable a hybrid Brain-Computer Interface for hand motor rehabilitation. Journal of NeuroEngineering and Rehabilitation, 20(1), 5.

[30] Vourvopoulos, A., Pardo, O. M., Lefebvre, S., Neureither, M., Saldana, D., Jahng, E., & Liew, S. L. (2019). Effects of a brain-computer interface with virtual reality (VR) neurofeedback: A pilot study in chronic stroke patients. Frontiers in human neuroscience, 13, 210.

[31] Saway, B. F., Palmer, C., Hughes, C., Triano, M., Suresh, R. E., Gilmore, J., ... & Rowland, N. C. (2024). The evolution of neuromodulation for chronic stroke: from neuroplasticity mechanisms to brain-computer interfaces. Neurotherapeutics, 21(3), e00337.

[32] Endzelytė, E., Petruševičienė, D., Kubilius, R., Mingaila, S., Rapolienė, J., & Rimdeikienė, I. (2025). Integrating Brain-Computer Interface Systems into Occupational Therapy for Enhanced Independence of Stroke Patients: An Observational Study. Medicina, 61(5), 932.

[33] Molinari, M., & Masciullo, M. (2020). Stroke and potential benefits of brain-computer interface. Handbook of Clinical Neurology, 168, 25-32.

[34] Mrachacz-Kersting, N., Jiang, N., Stevenson, A. J. T., Niazi, I. K., Kostic, V., Pavlovic, A., ... & Farina, D. (2016). Efficient neuroplasticity induction in chronic stroke patients by an associative brain-computer interface. Journal of neurophysiology, 115(3), 1410-1421.

[35] Lin, B. S., Chen, J. L., & Hsu, H. C. (2017). Novel upper-limb rehabilitation system based on attention technology for post-stroke patients: A preliminary study. IEEE Access, 6, 2720-2731.